Combined Use of Various Passive Radar Range-Doppler Techniques and Angle of Arrival using MUSIC for the Detection of Ground Moving Objects

Thomas Chan, Sermsak Jarwatanadilok, Yasuo Kuga, & Sumit Roy
Department of Electrical Engineering,
University of Washington, Seattle, WA 98195, USA
Email: tywc@u.washington.edu

Abstract:
The detection of ground moving targets, such as humans and ground vehicles is important for border security. Using the data received from a passive radar system, an algorithm was developed to pinpoint the location of ground moving objects over a fixed area. The algorithm combines the data from cross-correlation range-Doppler techniques with the data from angle of arrival MUltiple SIgnal Classification (MUSIC) techniques. The extracted time-delay values from the derived ambiguity function are converted into ellipse ranges and then joined with MUSIC's derived target angles; this information can then be processed into a 2-D image of scan area. The algorithm was tested with numerical simulations using different scenarios and test cases; these include the presence of some background clutter noise, the use of multiple sets of receivers, and the use of multiple sources. The system and algorithm was also tested experimentally using a 1 GHz cell phone antenna (emitting a BPSK signal) as the source, dipole antennas as the receivers, and a conducting cylinder as the target. This experiment was conducted in an outdoor environment to simulate noisy and realistic conditions. This report will provide a detailed analysis of the overall system, algorithm, and a summary of the results and findings of the numerical simulations and experimental tests.

1. Introduction

The ability to detect fast-traveling airborne vehicles using passive radars system have been studied at length by Howland, Yi, etc. [1, 2, 3]; however, less papers focus primary on the detection of ground objects using passive radars for the purpose of border security. This is because it is more difficult to perform Doppler analysis on slower moving targets in the presence of a constantly changing background environment. Many of the papers about passive radar object detection take a more traditional linear dynamics approach, such as using a Kalman Filter, for target tracking, which involves non-trivial analysis. Also, passive imaging in multiple scattering environments was studied by Wang et al [4], who uses an analytical approach by deriving the Point Spread Function (PSF) based on Green's Function calculations. In this paper, we describe a simpler theoretical imaged-based passive radar system, which combines the use of

cross-correlation techniques with the adaptive beamforming technique, MUltiple SIgnal Classification (MUSIC). The goal of this method is to improve the delectability of slowly moving ground objects, such as humans and ground vehicles, in a random cluttered background.

A standard passive radar, FM radio based, target detection system includes an FM transmitter, adaptive filtering, range-Doppler processing, and line tracking of moving target techniques using a Kalman Filter. Similarly, our system includes Least Mean Square (LMS) adaptive filtering and creating an amplitude-range-Doppler (APD) surface; the novelty is that these techniques are then combined with a high-resolution angle-of-arrival (AOA) technique called MUSIC [5]. Various techniques of radar imaging using adaptive array beamforming were also discussed in Curry's thesis [6]; subsequently, a MUSIC algorithm was developed to be used as the AOA detection scheme for our system.

2. System Overview

A block diagram of the processing algorithm is shown in Figure 1. Starting from the left side of the diagram, the total signal is collected from the surveillance array antenna, which consists of a set of array receivers, each $\lambda/2$ apart. There is also a reference antenna that collects the direct signal from the transmitter; these are used in the adaptive cancellation and Doppler processing steps. The adaptive filter is applied to the received signals from the array in order to reject the unwanted direct transmitter signal. The data after the cancellation is fed into a cross-correlation scheme that outputs APD surfaces to be processed; the time-delay values, which are later converted into range-ellipse, are extracted from these surfaces. The other target detection scheme is the AOA estimation, which uses the MUSIC algorithm that translates the collected data at the surveillance array antennas into a target location angle. By combining the range-ellipses with the MUSIC AOA, the target location can be approximated and imaged from the intersection of these two techniques. A more detailed analysis of each block component of the system is the sections below.

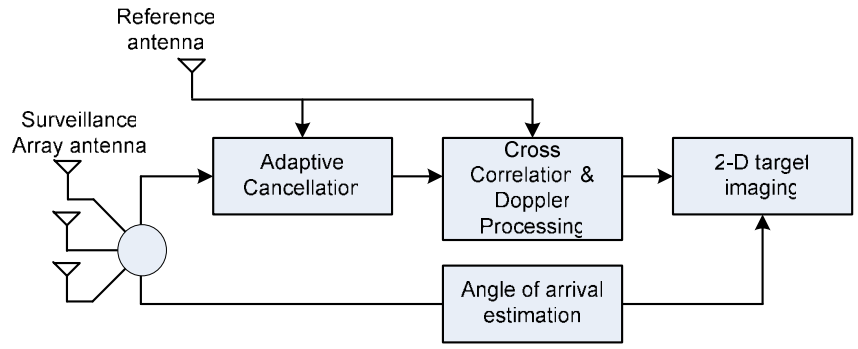

Figure 1: Block diagram of system

2.1 The Passive Radar Source and theoretical analysis

To optimize the efficiency of the system, it will require high-bandwidth passive radar signals, such as ones from DTV; however, a synthetic DTV signal has not yet been implemented as the source. Thus, currently our system was theoretically tested at 1 GHz, emitting a randomly generated 512 bit BPSK wave at a bit rate of 100 MHz (experimentally the bit rate is much lower). The AOA algorithm analyzes the modulated BPSK wave, while the correlation scheme processes the demodulated binary signal.

The theoretical array received signals are calculated using simple Rayleigh scattering; the received signals, which are reflected off the targets, are time-delayed versions of the source signal. When random noise particles are added to the background media, the same Rayleigh scattering is applied to these noise particles, but the reflectivity is set to 0.1. The target and noise signals received at each array are added together.

2.2 Adaptive Cancellation

The goal of an adaptive noise canceller is to remove the direct signal and clutter from the surveillance channels before the cross-correlation processes. The structure of our adaptive canceller is shown in Figure 2; r(n) is the signal from the reference channel, x(n) is the total signal from the surveillance arrays, $w_1(n)$ are the constantly updated direct signal values from the adaptive filter, e(n) is the true echo signal we are trying to derive (based on the subtraction of x(n) and $w_1(n)$). The adaptive filter used is a very simple LMS Update Algorithm [7] and can be summarized by Equations 1-3 below.

$$w_1(n) = conj(w) \cdot r(n) \quad (1)$$

$$e(n) = x(n) - w_1(n) \quad (2)$$

$$w = w + \mu \cdot x(n) \cdot conj(e(n)) \quad (3)$$

where 'w' is the constantly updated weight value and 'μ' is the step-size parameter that controls the convergence characteristics of the LMS algorithm. It was arbitrarily chosen as 0.02.

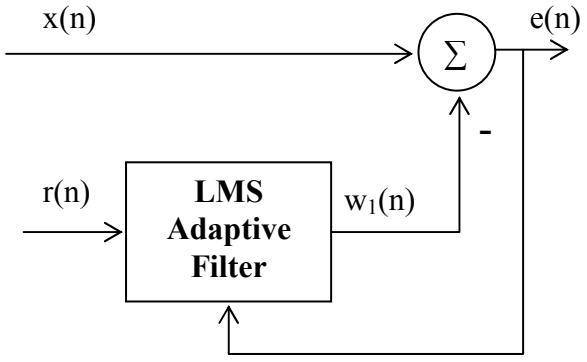

Figure 2: Adaptive noise canceller structure

2.3 Cross Correlation Target Detection

Range-Doppler estimation is a process that involves creating Doppler shifted time-delayed versions of the reference signal and cross-correlating that with the data from the surveillance antenna. The processing is also called the Ambiguity Function, which can be written in discrete time notation as seen in Equation 4.

$$\left|\psi(\tau,\upsilon)\right| = \left|\sum_{n=0}^{N-1} e(n)d^*(n-\tau)e^{j2\pi cn/N}\right| \qquad (4)$$

where Ψ is the ARD surface to calculate, e(n) is the filtered echo signal from the adaptive cancellation, d(n) is the reference signal, and τ is a time delay. The ambiguity function was implemented by calculating the discrete Fourier transform of e(n)d*(n-τ).

Typically, this technique is geared towards locating fast moving objects in the air, where a Doppler shift is detectable. Since we are dealing with slow moving ground objects, the Doppler shift part of the ARD will remain at zero and the only values that are important is the location of each target's time-delay peak. Figure 3 is an example which applies the cross-correlation scheme and ambiguity function equation on two targets, eventually generating an ARD surface. Two distinct time-delay peaks are noticeable.

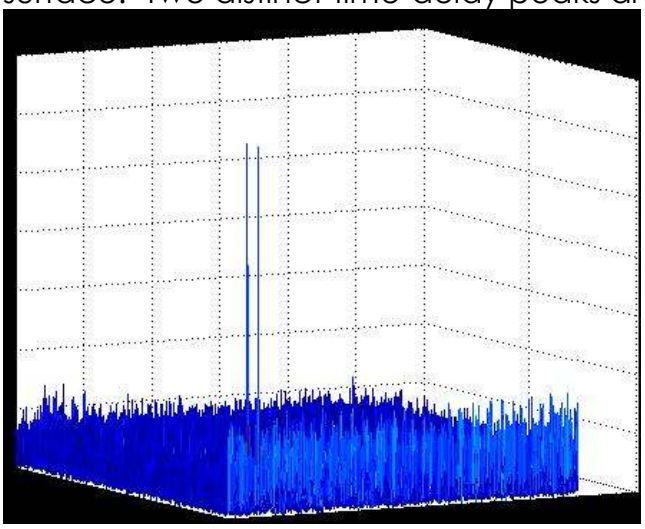

Figure 3: ARD surface with time-delay peaks for two targets

2.4 Angle of Arrival Detection MUSIC

The covariance matrix, R, is the collected data for each of the array receivers in the time-domain. To get better angular resolution and better distinguish between correlated signals with close AOAs, a special smoothing or sub-array averaging technique [8] is required; it works by dividing a full array into smaller arrays. This method can be used to resolve correlated arrivals; however, the tradeoff for using spatial averaging is that it leads to fewer degrees a freedom, which also leads to fewer targets that can be detected unless more arrays are added. For a full array of N elements, there are N-1 degrees of freedom; in sub-array averaging, if the size of the sub-array is Ns (Ns<N), then there are Ns-1

degrees of freedom. Figure 4 is an illustration of this technique and the modified covariance matrix equation is given by Equation 5.

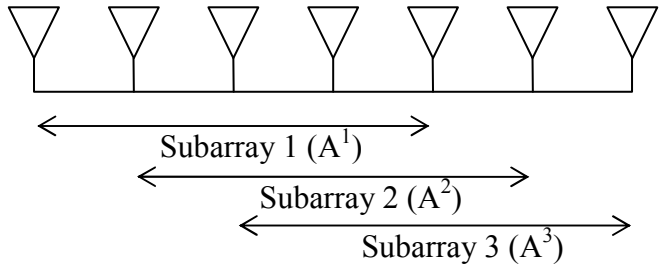

Figure 4: Subarray Spatial Smoothing

$$R = \frac{1}{M}\sum_{k=1}^{M} A^k A^{+k} \tag{5}$$

where A are the various sub-arrays and M is the total number of sub-arrays; A^+ is the conjugate and transpose of A. Once the updated covariance matrix is found, MUSIC is summarized by Equations 6 and 7; they can be used to extract the angle of arrival values and create the AOA plot.

$$\hat{\mathbf{R}}_{MUSIC}^{-1} = \sum_{i=Nz+1}^{M} \mathbf{v}_i \mathbf{v}_i^H \tag{6}$$

$$\mathrm{P}^{MUSIC} = \left[\mathbf{e}^H \hat{\mathbf{R}}_{MUSIC}^{-1} \mathbf{e}\right]^{-1} \tag{7}$$

where 'v' is the Single Value Decomposition (SVD) of R, found from Equation 5. The scanning vector, e, can be generalized for each array antenna and a range of θ values as

$$e^{j\cdot 2\pi\cdot\theta} \tag{8}$$

For the AOA plotting, the MUSIC algorithm will give beams at specific angle locations. Figure 5 is an example which uses the MUSIC algorithm to detect three targets. Ideally, the angle at the peaks of the beam should represent where the target should be located; however, this is not always the case, thus the angular resolution, $\Delta\theta$, is found at the 3dB points. When these angles are translated into multiple AOA lines on the 2-D image, this gives us more flexibility in terms of a possible area for target locations, not just an intersection point.

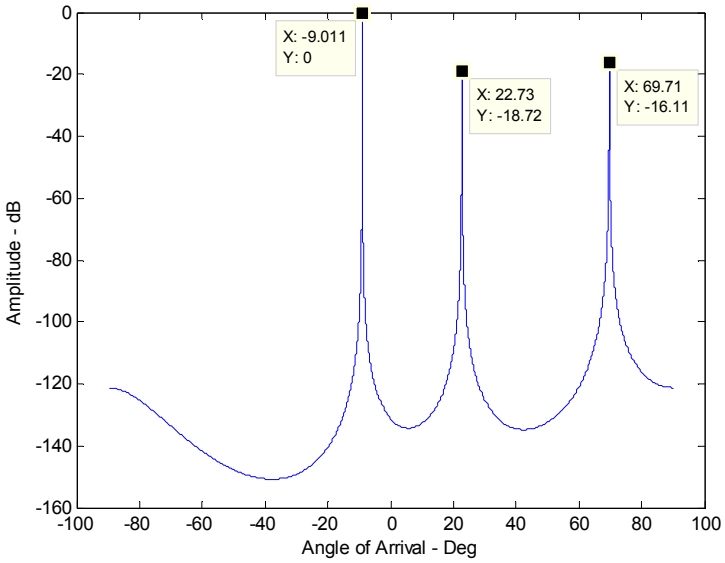

Figure 5: AOA using MUSIC

2.5 2-D Target Imaging

The target is imaged by finding the intersection between the range-ellipse created from the time-delay value extracted from the ARD. The range-ellipse is processed by analyzing Figure 6.

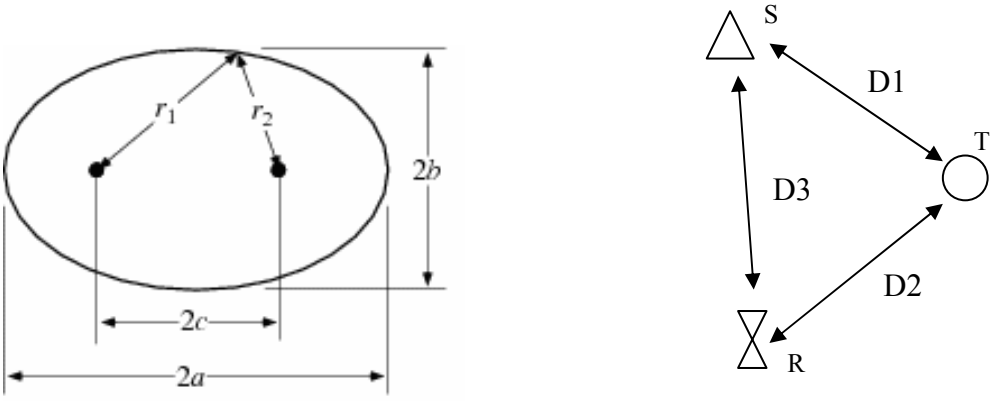

a) b)

Figure 6: a) General ellipse variable, b) source, target, receiver variables

The general equations for an ellipse (Figure 6a) is given by

$$r_1 + r_2 = 2 \cdot a \tag{9}$$

$$b^2 = a^2 - c^2 \tag{10}$$

The general equations for our system (Figure 6b) is given by:

$$td = \frac{(D1 + D2) - D3}{c} \tag{11}$$

$$D1 + D2 = td \cdot c + D3 \tag{12}$$

By combining Equations 9, 11, and 12, the 'a', 'b', and 'c' values corresponding to our system can be calculated, and subsequently, the range-ellipse can be imaged. By combining the range ellipses with the AOA plot lines, the intersection points represent the possible target locations.

3. Results and Analysis

3.1 Theoretical Simulations

Theoretically, we tested our algorithm with the parameters discussed in Section 2.1 with three different cases. Case 1 is with one source and one receiver; Case 2 is with one source with two sets of receivers; Case 3 is with two sources with one set of receivers. The goal of adding multiple sources and multiple receivers is to gain additional degrees of freedom, which gives us more information and accuracy to possible target locations. The theoretical results in free space for each of these cases is typically very accurate, thus, results shown in this section will also include a randomly generated set of 20 scattering particles, with 0.1 reflectivity as the background media. Only one target was tested for each case to avoid unnecessary image cluttering. The total area tested will be about 150 m-150 m for all cases. The triangle represents the

location of a transmitter, each 'x' on the plot is the location of the array receiver, and the red dot is the actual location of the target.

3.1.1 Case 1 - One Source, One Receiver

This is the simplest case, the transmitter is located at (5, 95) m; there is 7-array receiver whose spacing is λ/2 (at 1 GHz) and the middle receiver is located at (20.45, 0) m; the target is located at (70, 120) m. Figure 7 is the free space case; in Figure 8, 20 randomly located noise particles are added to act as background clutter. The resolution of the range-ellipses is 3m; this value is strictly dependent on the source bandwidth (100 MHz). This is why a using high-bandwidth transmitter is critical.

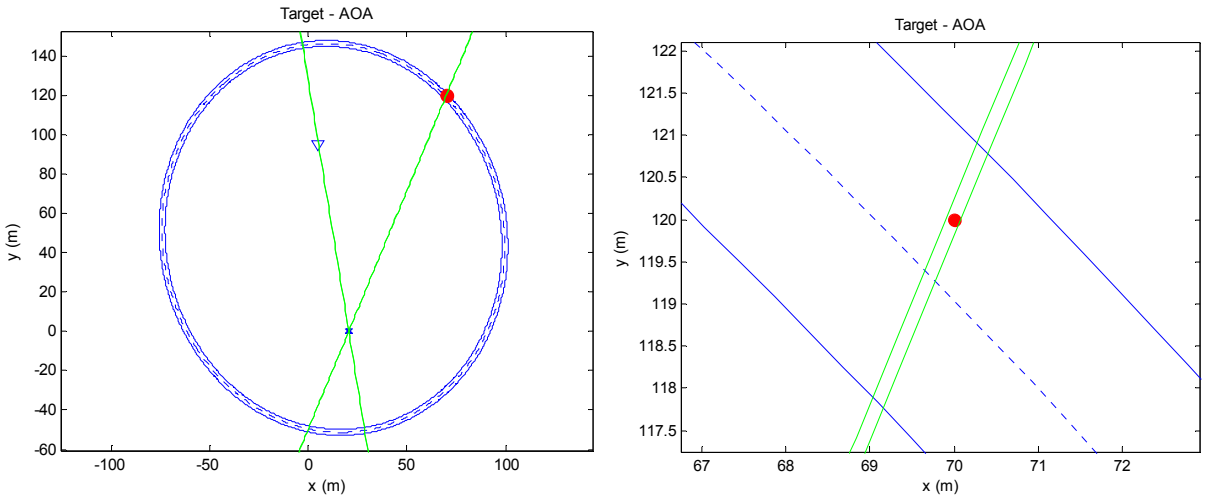

Figure 7: Case 1 free space 2-D image plot

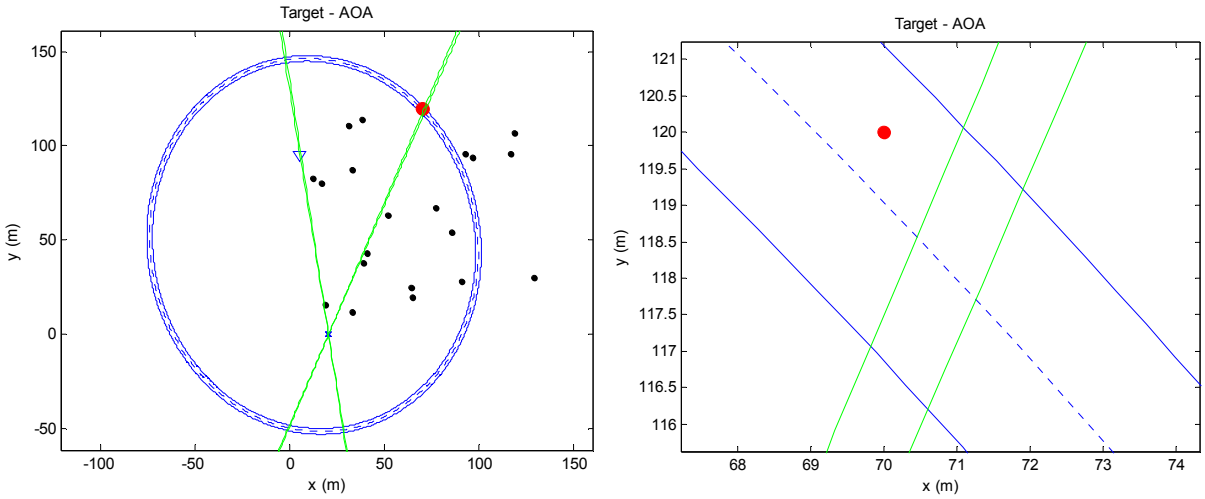

Figure 8: Case 1 2-D image plot with 20 random particles

3.1.2 Case 2 - One Source, Two Receivers

For this case, the transmitter, receivers, and target are all located at the same places as Case 1, except a new set of 7 receivers that are added vertically on

the right side, where the middle receiver is located at (140, 60.45) m. Figures 9 and 10 are the free space and noisy cases, respectively.

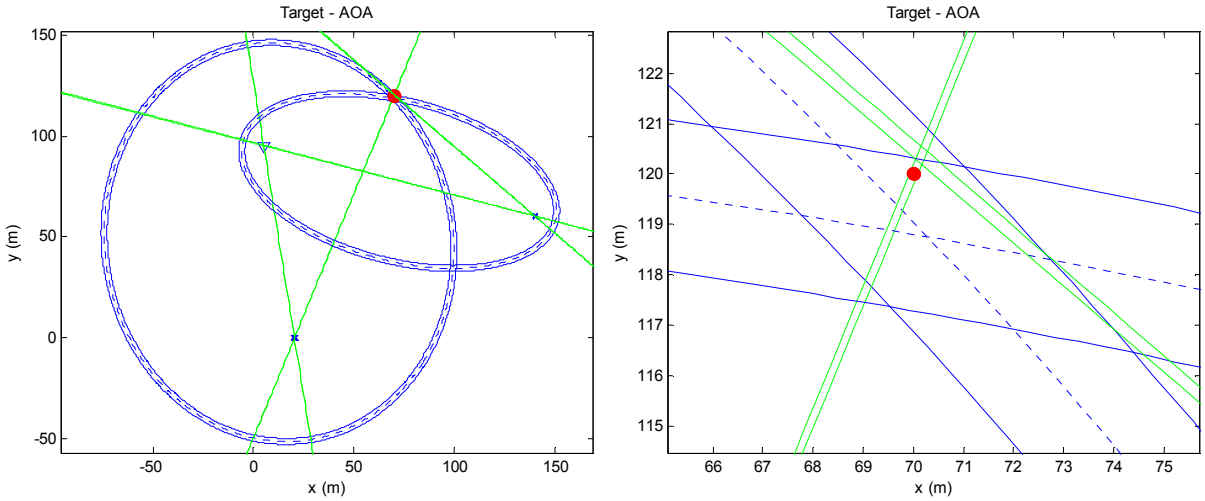

Figure 9: Case 2 free space 2-D image plot

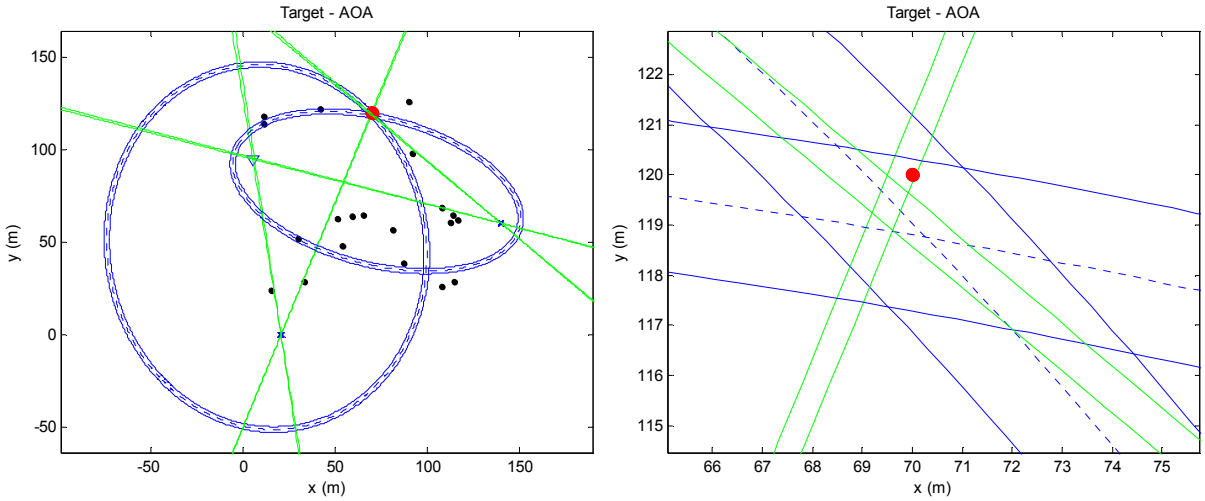

Figure 10: Case 2 2-D image plot with 20 random particles

3.1.3 Case 3 - Two Sources, One Receiver

For this case, the transmitter, receivers, and target are all located at the same places as Case 1, except another transmitter is located at (110, 70) m. The received signal from each transmitter is analyzed and processed independently through our system, and data from each is then combined in the 2-D image. Figures 11 and 12 are the free space and noisy cases, respectively.

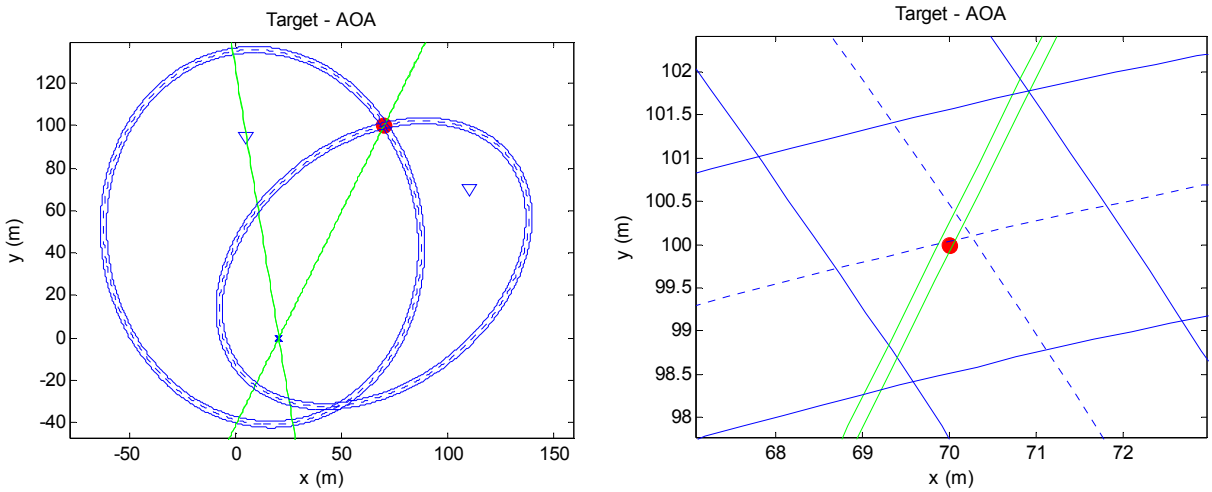

Figure 11: Case 3 free space 2-D image plot

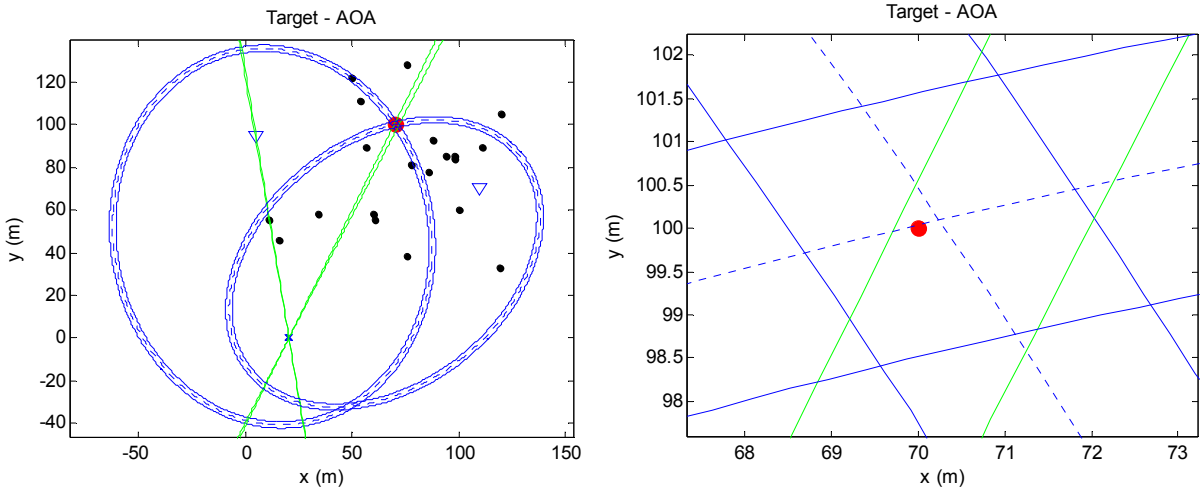

Figure 12: Case 3 2-D image plot with 20 random particles

Sometimes the accuracy of both the AOA MUSIC algorithm and the range-Doppler ellipses slightly drops when noise particles of 0.1 reflectivity are added. This is not always the situation though, as sometimes adding random particles have little effect on the AOA estimation; it largely depends on the number of random noise particles and where they are located relative to the target. This is why in some instances, depending on the nature of the background noise, one image is sometimes not sufficient in pinpointing exact target location. Thus, if we collate the data from the different still images of a moving target, we can combine all the information from these images to get a more accurate idea of where the slowly moving ground object is located. Further in-depth analysis of the collection of still image data should also give us information about the direction the target is going and how fast it is traveling.

3.2 Experimental Testing

The experimental approach involves random binary bit sequence generated in Matlab, Figure 13, which can be uploaded onto an arbitrary function generator. The source bandwidth was significantly lowered because the 100 MHz that was used in theoretical analysis is hard to implement experimentally; also the number of bits was lowered from 512 to 30 to simplify the analysis. Thus, the binary signal contains 30 bits, has a 10 MHz bit rate and sampled at 250 MSa/s, for a total of 750 points. Then, a mixer is used to multiply the generated binary signal on the function generator with a 1-GHz oscillating wave, with the output being the desired modulated wave. The modulated wave is emitted into free space via a 1 GHz cell phone antenna.

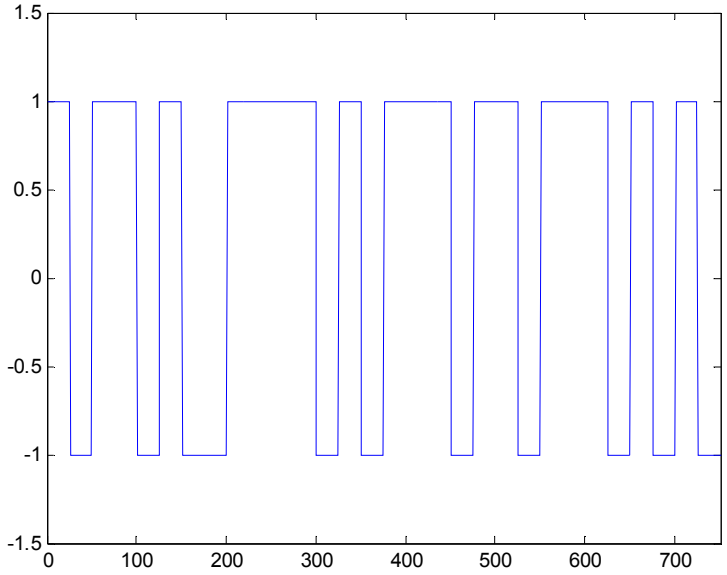

Figure 13: Input binary bit sequence

The signals will be received from four λ/2 dipole antennas that are λ/2 spaced apart. The signals received from this antenna are then fed into another mixer to be multiplied with a 1-GHz oscillating wave (synchronized to the original), with the output being a 10 MHz down-converted modulated wave. An oscilloscope is used to extract these signals to be post-processed where we can implement our algorithm. Figure 14 are snapshots of some of the source and receiver experimental equipment that is used.

Figure 14: Snapshots of equipment

3.2.1 Experimental Setup

Combining the source and receiver elements described above, we can create a set-up similar to the theoretical analysis of Case 1 (Section 3.1.1), but on a slightly smaller scale (25x25 meter area) and using a conducting cylinder as the target. Also, instead of a reference receive antenna used to acquire the direct signal from the source, a long wire is used to connect the binary signal from the function generator directly to the scope, which will temporarily serve as the reference signal. An additional wire is needed to synchronize the 1 GHz local oscillators. Figure 15 shows the desired setup (not drawn to scale).

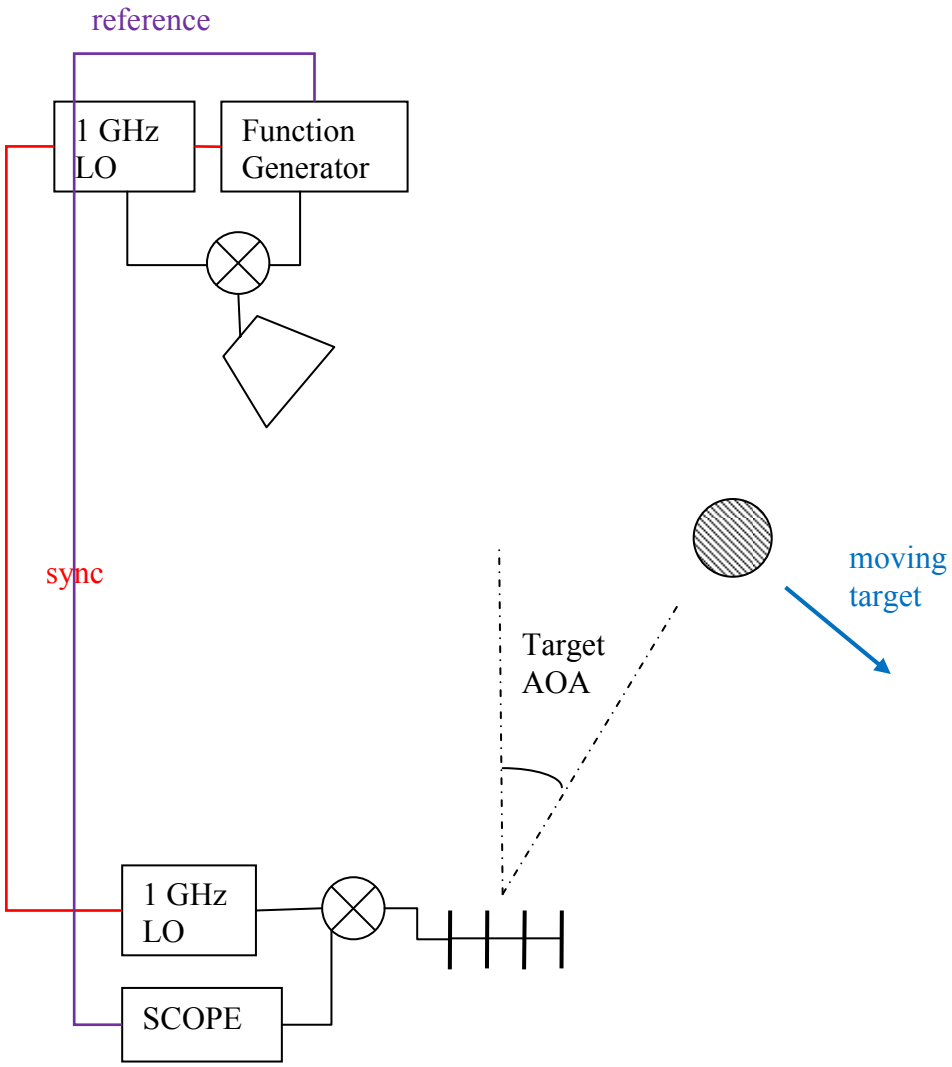

Figure 15: Outdoor experimental setup with target

3.2.2 Theoretical Testing of Experimental Setup

Figure 16 shows the theoretical setup with the desired locations of the source target and receiver. The four receivers are located at (2,1) m, (2.15,1) m, (2.3,1) m, & (2.45, 1) m. The target will be stationary at (10, 15) m and will be moved 1m to the right and 1m down until (15, 10) m to simulate a moving object. The antenna source is located at (1, 24) m. These are exact locations based off ideal theoretical conditions; the locations will likely change based on testing environment.

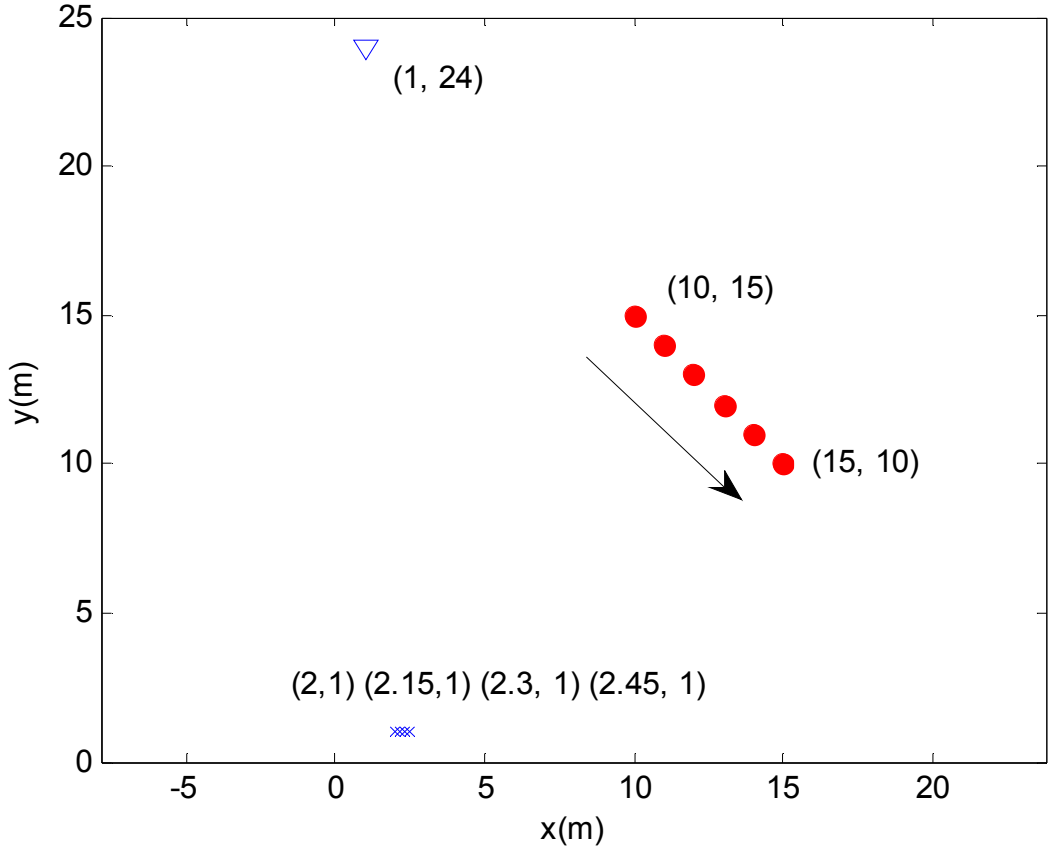

Figure 16: Theoretical setup with desired receiver, transmitter, and target locations

Figures 17-20 shows some of the results based on the theoretical simulation based on the MUSIC and correlation algorithms. The resolution of the range ellipses was not included because of the small bandwidth (10 MHz→30m resolution), and the 3-dB resolution of the AOA angles is not included because sub-array averaging is needed for reasonable angular resolution and this technique is not used because we only have four receiver antennas.

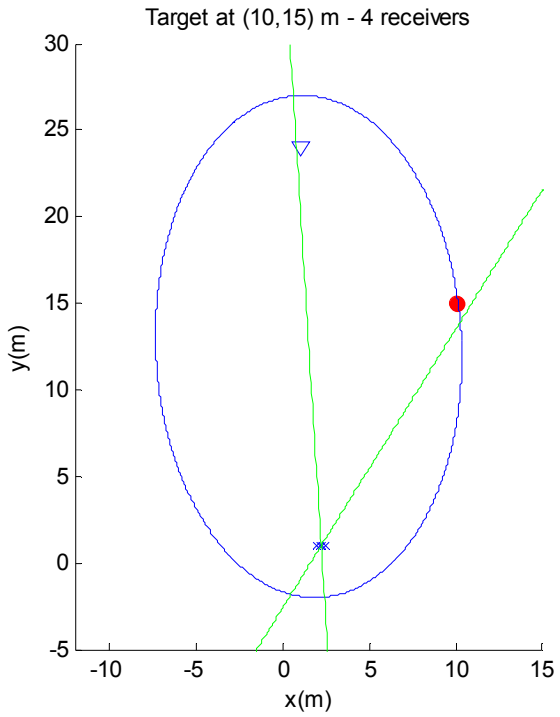

Figure 17

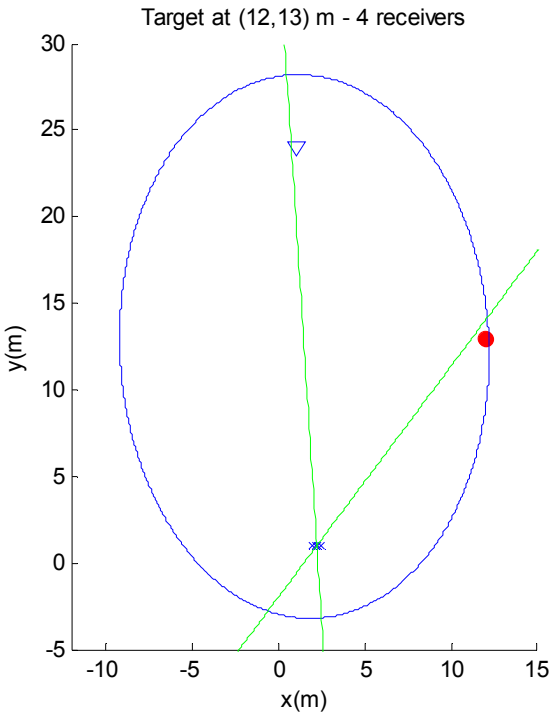

Figure 18

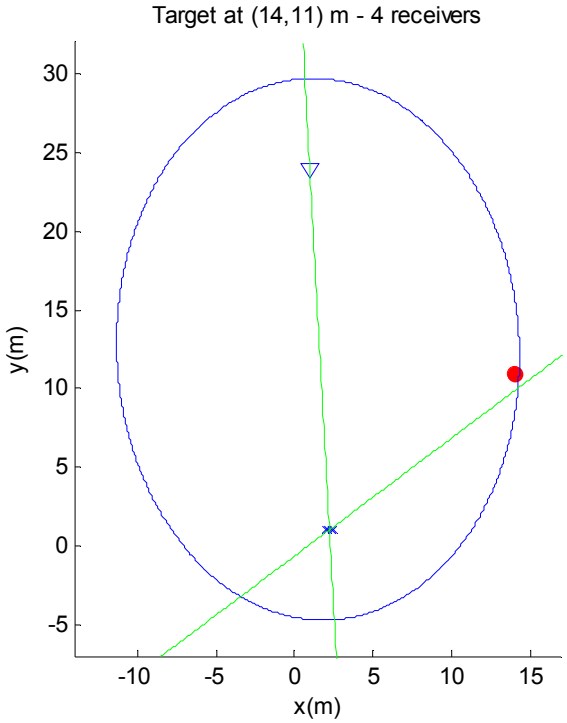

Figure 19

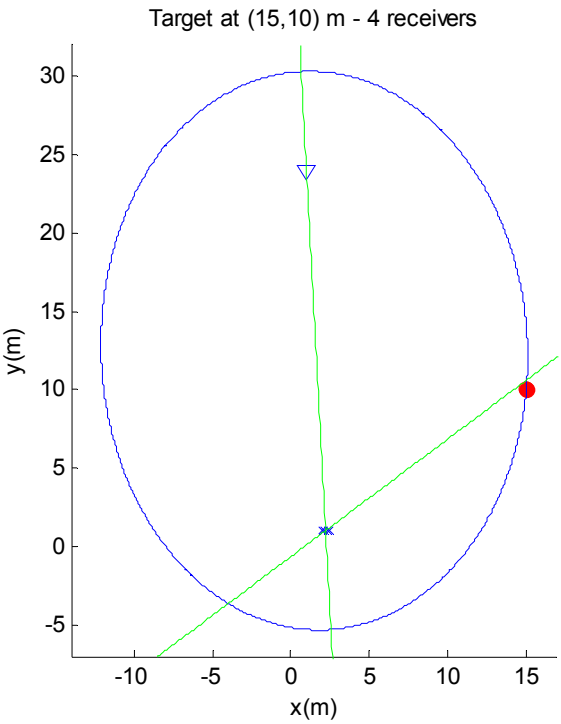

Figure 20

3.2.3 Experimental Results

To be added…

References

[1] P.E. Howland and M. Ceng. "Target tracking using television-based bistatic radar," *IEE Proceedings* online no. 19990322, February 1999.
[2] Z.J.H. Yi and T. Ling. "Adaptive Beamforming Passive Radar Based on FM Radio Transmitter," *IEEE*, 2006.
[3] P.E. Howland, D. Maksimiuk, and G. Reitsma. "FM radio based bistatic radar," IEE Proceedings of Radar, Sonar and Navigation, vol. 152, pp. 107-115, 2005.
[4] L. Wang, I.Y. Son, and B. Yazici. "Passive imaging using distributed aperatures in multiple scattering environments," IOP Publishing Ltd, May 7 2010.
[5] R. O. Schmidt. "Multiple emitter location and signal parameter estimation," *Proc. RADC Spectral Estimation Workshop*, Rome, NY, pp. 243–258, 1979.
[6] Mark A. Curry. "Techniques for Radar Imaging Using A Wideband Adaptive Array," University of Washington Doctoral Thesis, pp. 10-32, 2001.
[7] KK Shetty. "Chapter 6 – Least Mean Square Algorithm," Florida State thesis, pg. 55-65, 2004.
[8] T.J. Shun, M. Wax and T. Kailath. "On Spatial Smoothing for Direction-of-Arrival Estimation of Coherent Signals," *IEEE Transactions on Acoustics, Speech, and Signal Processing*, vol. ASSP-33, NO. 4, pp. 806-811, August 1985.